

BIORTHOGONAL RATIONAL KRYLOV SUBSPACE METHODS*

NIEL VAN BUGGENHOUT[†], MARC VAN BAREL[†], AND RAF VANDEBRIL[†]

Abstract. A general framework for oblique projections of nonhermitian matrices onto rational Krylov subspaces is developed. To obtain this framework we revisit the classical rational Krylov subspace algorithm and prove that the projected matrix can be written efficiently as a structured pencil, where the structure can take several forms, such as Hessenberg or inverse Hessenberg. One specific instance of the structures appearing in this framework for oblique projections is a tridiagonal pencil. This is a direct generalization of the classical biorthogonal Krylov subspace method where the projection becomes a single nonhermitian tridiagonal matrix and of the Hessenberg pencil representation for rational Krylov subspaces. Based on the compact storage of this tridiagonal pencil in the biorthogonal setting, we can develop short recurrences. Numerical experiments confirm the validity of the approach.

Key words. Rational Krylov, Biorthogonal, Short Recurrence, Oblique Projection, Matrix Pencil

AMS subject classifications. 15A22, 47A75, 65F99, 65Q30

1. Introduction. Krylov subspace methods, introduced by A. N. Krylov [18], are an indispensable tool in science and engineering for transforming large datasets to manageable sizes. There is an enormous amount of variants of Krylov subspace methods. A good overview can be found in the books of Saad [28], van der Vorst [33], and Gutknecht [15]. In this article we focus on a particular type of Krylov subspace methods, namely the rational Krylov subspace methods in a non-orthogonal, but oblique projection process. This allows to save the projected matrix as two tridiagonal matrices, which is a more data-sparse representation compared to the Hessenberg pair arising from orthogonal projection.

Rational Krylov subspaces were introduced by Ruhe [25] illustrating that faster convergence could be obtained when, e.g., approximating non-dominating eigenvalues [26] and constructing a reduced-order model for dynamical systems [11–13].

Arnoldi [2] linked Hessenberg matrices to the orthogonal basis stemming from a Krylov subspace and developed an iteration to build up these bases. Iterative construction of matrices involved in biorthogonal Krylov subspace methods are due to Lanczos [19], where an oblique projection results in a tridiagonal matrix. Even though the oblique projection process is less stable than the classical orthogonal projection, there is a significant gain in memory storage and computing time. A nice introduction into biorthogonal Krylov subspace methods is provided by Saad [27]. The most popular biorthogonal method for solving systems of equations is the BiCGStab method of van der Vorst [32].

Biorthogonal Krylov subspace methods for rational Krylov subspaces have been described only partially in literature [11–13]. This article will generalize previous results and provide a general framework. We will prove that the oblique projection linked to biorthogonal rational Krylov subspaces results in a matrix pencil, of which both matrices can be chosen to be tridiagonal, possibly nonhermitian. The highly structured pencil allows us to develop a short recursion to compute the biorthogonal bases and the projected pencil. To derive these results we first need to reconsider the structure of the orthogonally projected matrix linked to a classical rational Krylov subspace. We prove that instead of the single rational Hessenberg

*Submitted to the editors ..., 2018

[†]Department of Computer Science, KU Leuven, University of Leuven, 3001 Leuven, Belgium. (raf.vandebril@kuleuven.be, niel.vanbuggenhout@kuleuven.be, marc.vanbarel@kuleuven.be)

The research of the authors was supported by the Research Council KU Leuven, C1-project (Numerical Linear Algebra and Polynomial Computations), by the Fund for Scientific Research–Flanders (Belgium), EOS Project no 30468160, and by the Research Council KU Leuven: C14/16/056 (Inverse-free Rational Krylov Methods: Theory and Applications)

40 matrix we can also work with a pair of matrices of particular structure, such as Hessenberg or
 41 inverse Hessenberg.

42 Gutknecht studied short recursions, (k, l) -step methods for fixed point equations [14, 16],
 43 by means of a Hessenberg-triangular pencil. Some classical Krylov subspace methods can
 44 be described by (k, l) -step methods, e.g., BiCG is a $(2, 1)$ -step method. The biorthogonal
 45 rational Lanczos method introduced here does not immediately fit this framework.

46 Some notable results are provided below, which are in some sense special cases of the
 47 general framework provided here. We discuss which spaces are used and what structure the
 48 projection onto these subspaces exhibits.

49 Using orthogonality of Laurent polynomials, Jagels and Reichel [17] constructed a
 50 recurrence for extended Krylov subspaces with regularity in the poles (a repetition of $i \geq 1$
 51 times A and one time A^{-1}) and a symmetric matrix A . They represented their projected
 52 matrix as a single matrix. Schweitzer [29] constructed in a similar way a nonsymmetric
 53 Lanczos iteration for extended Krylov subspaces, only valid when a negative and positive
 54 power is alternated in both spaces. Gallivan, Grimme and Van Dooren derived a nonsymmetric
 55 rational Lanczos iteration [12]. They use the same poles in both subspaces and represent
 56 the projection as a pencil, which is a tridiagonal pencil, except for some off-diagonal fill-in
 57 when a change of pole occurs. Watkins [36] provided the first elegant representation of the
 58 AGR/CMV-factorization [1, 6, 9, 30, 36] as a matrix pencil, for a nice overview of the history
 59 we refer to the paper by Simon [30]. This factorization is in fact also a biorthogonal relation,
 60 but for unitary matrices.

61 Some elementary results are provided in Section 2, with a focus on sparsity and low-
 62 rank structure. Section 3 discusses rational Krylov subspace methods and the structure of
 63 the projection. Section 4 deals with biorthogonal rational Krylov subspace methods and
 64 an overview presenting all possible structures. In Section 5 a rational Lanczos iteration is
 65 derived based on the tridiagonal pencil structure, some numerical experiments are performed
 66 illustrating the validity of the approach.

67 **2. Basics.** Since this text will rely on matrix computations and the main results involve
 68 sparsity and low-rank structure, this section is devoted to these types of structure (structure
 69 will refer from now on to both sparsity and low-rank structure). Useful elementary results
 70 for standard Krylov subspace methods are repeated in Section 2.1. For more details see, e.g.,
 71 [20, 24, 27]. Using the QR-factorization we introduce inv-Hessenberg, extended Hessenberg
 72 and rational Hessenberg matrices in Section 2.2.

2.1. Standard Krylov subspaces. Standard Krylov subspace methods perform an or-
 thogonal projection of some matrix $A \in \mathbb{C}^{m \times m}$ onto the Krylov subspace

$$\mathcal{K}_n(A, v) = \text{span}\{v, Av, A^2v, \dots, A^{n-1}v\},$$

73 with a starting vector $v \in \mathbb{C}^m$, $\|v\|_2 = 1$. Note that these subspaces are nested, i.e., $\mathcal{K}_{n-1} \subseteq$
 74 \mathcal{K}_n . Using the Arnoldi iteration [2] a *nested* orthonormal basis V_n for \mathcal{K}_n can be iteratively
 75 constructed together with the projection onto the lower dimensional subspace $\mathcal{K}_{n-1}(A, v)$:
 76 $V_{n-1}^H A V_{n-1} = H_{n-1} \in \mathbb{C}^{(n-1) \times (n-1)}$.

77 A basis $V_n \in \mathbb{C}^{m \times n}$ for a subspace \mathcal{S}_n of dimension n is called *nested* if $\mathcal{S}_1 \subseteq \mathcal{S}_2 \subseteq \mathcal{S}_3 \subseteq \dots$,
 78 where \mathcal{S}_i is spanned by the first i columns of V_n . The projected matrix H_n has upper-
 79 Hessenberg structure, i.e., $h_{i,j} = 0$ for $i > j + 1$, where $h_{i,j}$ denotes the element on the i th
 80 row and j th column of H_n . An alternative notation that will be used is $(H_n)_{i,j}$. In general
 81 H_n exhibits no particular structure above its diagonal.

82 **REMARK 2.1.** Throughout this text we assume that no breakdowns occur, i.e., no
 83 subdiagonal element $h_{i+1,i}$ of the projection $H_{i+1} = V_{i+1}^H A V_{i+1}$ is zero. Since, a zero

84 would imply that the subspace \mathcal{K}_i is invariant under multiplication with A or in other words
 85 $AK_i = \mathcal{K}_i$. Here every occasion where it is impossible to expand the current subspace \mathcal{S}_i , i.e.,
 86 $\mathcal{S}_{i+1} = \mathcal{S}_i$ will be called a breakdown. Typically a breakdown is a lucky event, i.e., lucky
 87 termination and we will therefore not focus on it. Serious breakdowns can also occur, see
 88 Gutknecht [15] and references therein for details.

89 For a full reduction, i.e., $n = m$ the subscripts are dropped $V^H AV = H$, $H \in \mathbb{C}^{m \times m}$.
 90 The structure of H_n can be represented as shown in Figure 2.1, where $\text{struct}(M)$ of some
 91 matrix M shows generic nonzero elements as \times and omits the zeros. In case of a Hermitian
 92 matrix $A^H = A$, the orthogonal projection onto $\mathcal{K}_n(A, v)$ results in a Hermitian Hessenberg
 93 matrix $V_n^H AV_n = T_n$. Or in other words it has Hessenberg structure both above and below
 94 its diagonal and is therefore tridiagonal, which is shown in Figure 2.1. Since we assumed no
 95 breakdowns, the Hessenberg and tridiagonal matrix are both *proper*, i.e., no zeros appear on
 the subdiagonal.

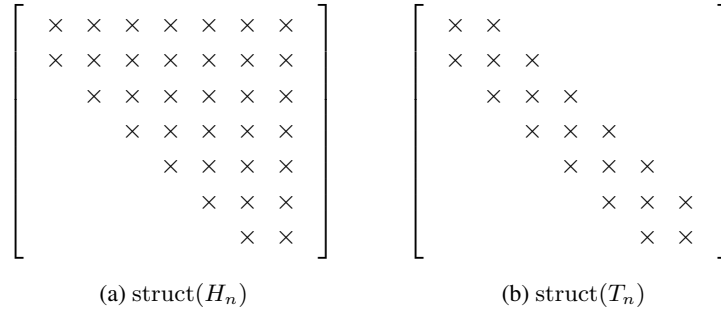


Fig. 2.1: Generic nonzero elements of a Hessenberg matrix H_n and tridiagonal matrix T_n are shown as \times .

96

2.2. Sparsity and low-rank structure. The sparsity that a Hessenberg matrix exhibits below its diagonal is also contained in its QR-factorization. The QR-factorization decomposes a matrix into the product of a unitary matrix Q and upper-triangular matrix R . To discuss the QR-factorization of a Hessenberg matrix we require core transformations. *Core transformations* in this text will refer to unitary matrices C_i that equal the unit matrix with a 2×2 unitary block embedded on the diagonal starting in row and column i :

$$C_i = \begin{bmatrix} I_{i-1} & & & \\ & \times & \times & \\ & \times & \times & \\ & & & I_{n-i-1} \end{bmatrix},$$

97 where C_i is of size $n \times n$ and I_k denotes the unit matrix of size $k \times k$. To compactly visualize a
 98 core transformation C_i , the notation $\begin{smallmatrix} \updownarrow \\ i \end{smallmatrix}$ will be used, with the top arrow pointing to row i
 99 and the bottom arrow pointing to row $i + 1$. Multiplication from the left with a core transformation
 100 $C_i: C_i M$, only affects the i th and $(i + 1)$ th rows of the matrix M .

101

102 **LEMMA 2.2** (QR-factorization of Hessenberg matrices). *Consider a proper upper-*
 103 *Hessenberg matrix $H \in \mathbb{C}^{n \times n}$, $h_{i,j} = 0$ for $i > j + 1$, the QR-factorization of H can be*

104 written as $H = C_1 C_2 \cdots C_{n-1} R$, where the C_i are nontrivial core transformations.

105

106 We will refer to $C_1 C_2 \cdots C_{n-1}$ as a *descending pattern* of core transformations. In
 107 case of an *ascending pattern* $Q = C_{n-1} \cdots C_2 C_1$, QR forms an *inv-Hessenberg matrix*.
 108 Inv-Hessenberg matrices have a low-rank structure below their diagonal similar to the structure
 109 of inverse Hessenberg matrices. We distinguish them from inverse Hessenberg matrices, since
 110 they do not have to be invertible. More details can be found in, e.g., the book by Vandebriil et
 111 al. [35], where they are called Hessenberg-like matrices.

112 Now a logical next step is to look at the structure of $Z = QR$ if the shape (the ordering
 113 of core transformations) contains ascending and descending patterns, i.e., a permutation of
 114 $C_1 C_2 \cdots C_{n-1}$. To be able to discuss this we note that $C_i C_j = C_j C_i$, for $|i - j| > 1$.
 115 Whenever a descending pattern $C_i C_{i+1}$ occurs, a Hessenberg block is formed and whenever
 116 an ascending pattern $C_{i+1} C_i$ occurs, an inv-Hessenberg block is formed.

117 **EXAMPLE 2.3.** Take, for example, $Q = C_1 C_4 C_5 C_6 C_3 C_2$, corresponding to the shape



118 The structure of $Z = QR$ is visualized similarly as by Mertens and Vandebriil [23] in Figure
 119 2.2. The dashed and dotted lines highlight the structure.

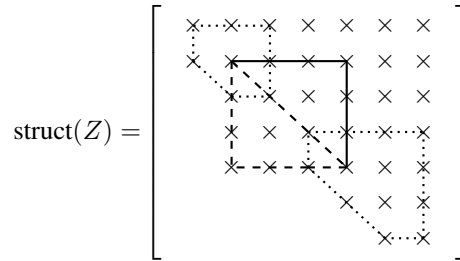


Fig. 2.2: Extended Hessenberg matrix Z obtained by a shape of core transformations $Q = C_1 C_4 C_5 C_6 C_3 C_2$, such that $Z = QR$.

120

121 From the structure in Figure 2.2 and the corresponding shape of Q it is clear that
 122 $C_1 C_2$ forms a Hessenberg block $Z_{1:3,1:3}$ (indicated by a dotted line), $C_4 C_3 C_2$ forms a
 123 inv-Hessenberg block $Z_{2:5,2:5}$ (low rank part indicated by a dashed line) and $C_4 C_5 C_6$ forms
 124 again a Hessenberg block $Z_{4:7,4:7}$.

125

126 A matrix containing both ascending and descending patterns of core transformations will
 127 be referred to as an extended Hessenberg matrix and links to the projection onto an extended
 128 Krylov subspace [34], which is a special case of a rational Krylov subspace.

129 **3. Rational Krylov subspaces.** Rational Krylov subspaces [25] will be denoted by
 130 $\mathcal{K}(A, v; \Xi)$, where A and v are defined as before and poles $\Xi = \{\xi_1, \xi_2, \dots\}$, with $\xi_k \in$

$\bar{\mathbb{C}} = \{\mathbb{C} \cup \infty\}$. If the k th pole is finite, a shift-invert operator $(\nu_k A - \mu_k I)^{-1}$ expands the subspace $\mathcal{K}_k(A, v, \{\xi_i\}_{i=1}^{k-1})$. The ratio $\mu_k/\nu_k = \xi_k$, which is the k th pole. We call this a pole since it is the pole of the shift-invert operator $(A - \xi_k I)^{-1}$. If the k th pole is infinite, multiplication with A expands the subspace. First the single-matrix representation of the orthogonal projection onto a rational Krylov subspace is considered in Section 3.1 and afterwards the pencil representation of this projection is discussed in Section 3.2 for a Hessenberg pencil, and in Section 3.3 for an inv-Hessenberg pencil.

3.1. Single-matrix representation. Consider an orthonormal nested basis $V_n \in \mathbb{C}^{m \times n}$ for $\mathcal{K}_n(A, v; \Xi)$, with $A \in \mathbb{C}^{m \times m}$, $v \in \mathbb{C}^m$ and given poles Ξ . Orthogonally projecting the matrix A onto \mathcal{K}_n and expressing the result using a single matrix Z_n provides the equation

$$(3.1) \quad V_n^H A V_n = Z_n.$$

The structure of the *rational Hessenberg matrix* Z_n can be deduced from the choice of poles. It allows for a factorization as $Z_n = QR + D$, where QR forms an extended Hessenberg matrix and D is a diagonal matrix containing the poles of the corresponding rational Krylov subspace [8]. Expansion using a shift-invert operator (finite pole) leads to an inv-Hessenberg block and expansion using multiplication with A (infinite pole) leads to a Hessenberg block [3]. Example 3.1 illustrates this.

EXAMPLE 3.1. Consider the extended Krylov subspace corresponding to the example from before $Z = C_1 C_4 C_5 C_6 C_3 C_2 R$, shown in Figure 2.2,

$$\mathcal{K}_7 = \text{span}\{v, Av, A^{-1}v, A^{-2}v, A^2v, A^3v, A^4v\}.$$

The corresponding poles are $\Xi = \{\infty, 0, 0, \infty, \infty, \infty\}$.

If the poles are chosen as $\Xi = \{\infty, \xi_2 = \frac{\mu_2}{\nu_2}, \xi_3 = \frac{\mu_3}{\nu_3}, \infty, \infty, \infty\}$, the space constructed is

$$\text{span}\{v, Av, (\nu_2 A - \mu_2 I)^{-1}v, (\nu_2 A - \mu_2 I)^{-1}(\nu_3 A - \mu_3 I)^{-1}v, A^2v, A^3v, A^4v\}$$

and the decomposition becomes $Z = QR + D$ as shown on figure 3.1, where ξ_2 and ξ_3 are the poles and the remaining elements of D can be chosen freely.

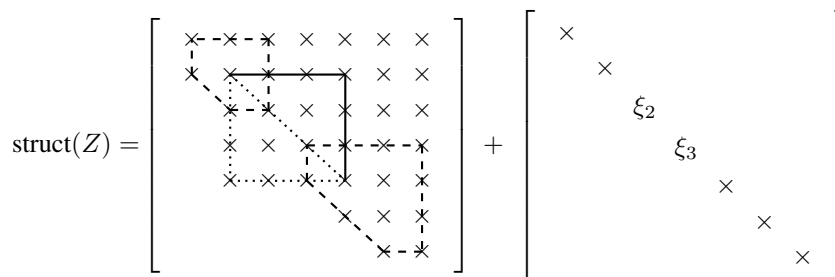


Fig. 3.1: Rational Hessenberg matrix Z corresponding to the projection onto $\mathcal{K}(A, v; \Xi)$ from Example 3.1, with $\Xi = \{\infty, \xi_2, \xi_3, \infty, \infty, \infty\}$.

The structure of the single-matrix representation can be explained through its link with the Hessenberg pencil representation discussed in Section 3.2, see Camps et al. [8].

3.2. Pencil representation. A pencil representation of the projected matrix onto a rational Krylov subspace can be constructed via an Arnoldi iteration. Theorem 3.2 provides the

153 rational Arnoldi iteration in its most general form, i.e., expansion of the subspace is done with
 154 the operator $(\nu_k A - \mu_k I)^{-1}(\rho_k A - \eta_k I)$.

THEOREM 3.2 (Rational Arnoldi iteration [25]). *Consider a matrix $A \in \mathbb{C}^{m \times m}$ and an orthonormal nested basis V_n for a rational Krylov subspace $\mathcal{K}_n(A, v; \Xi_n)$, where $\Xi_n = \{\xi_1, \xi_2, \dots, \xi_{n-1}\} \in \bar{\mathbb{C}}$. The recurrence relation to obtain a basis V_{n+1} for $\mathcal{K}_{n+1}(A, v; \Xi_{n+1})$, with $\Xi_{n+1} = \{\Xi_n, \xi_n\}$, in matrix form equals*

$$AV_{n+1}\underline{K}_n = V_{n+1}\underline{H}_n,$$

155 with \underline{H}_n and \underline{K}_n Hessenberg matrices of size $(n+1) \times n$. The ratio of their subdiagonal
 156 elements equals the poles of the rational Krylov subspace $\frac{(\underline{K}_n)_{k+1,k}}{(\underline{H}_n)_{k+1,k}} = \xi_k$, $k = 1, 2, \dots, n$.

157 *Proof.* Consider the formula for expanding the Krylov subspace $\mathcal{K}_k(A, v; \Xi)$ by multipli-
 158 cation with $(\nu_k A - \mu_k I)^{-1}(\rho_k A - \eta_k I)$, the subspace is invariant under the shift operator
 159 $(\rho_k A - \eta_k I)$. Afterwards orthogonalization with respect to all vectors in the current basis
 160 $V_k = [v_1 \ v_2 \ \dots \ v_k]$ is done using h_{ik} , $i = 1, \dots, k$ and normalization using $h_{k+1,k}$.
 161 This leads to a Gram-Schmidt orthogonalization procedure

$$(3.2) \quad h_{k+1,k}v_{k+1} = (\nu_k A - \mu_k I)^{-1}(\rho_k A - \eta_k I)v_k - h_{1k}v_1 - \dots - h_{kk}v_k.$$

Rewriting (3.2) reveals the k th column of matrices \underline{H}_k and \underline{K}_k

$$\begin{aligned} (\nu_k A - \mu_k I)h_{k+1,k}v_{k+1} &= (\rho_k A - \eta_k I)v_k - (\nu_k A - \mu_k I) \sum_{i=1}^k h_{ik}v_i \\ \nu_k A h_{k+1,k}v_{k+1} + \nu_k A \sum_{i=1}^k h_{ik}v_i - \rho_k A v_k &= -\eta_k v_k + \mu_k \sum_{i=1}^k h_{ik}v_i + \mu_k h_{k+1,k}v_{k+1} \\ A \left((\nu_k \sum_{i=1}^{k+1} h_{ik}v_i) - \rho_k v_k \right) &= \mu_k \left(\sum_{i=1}^{k+1} h_{ik}v_i \right) - \eta_k v_k \\ A \nu_k [v_1 \ \dots \ v_k \ v_{k+1}] \begin{bmatrix} h_{1k} \\ \vdots \\ h_{kk} - \rho_k/\nu_k \\ h_{k+1,k} \end{bmatrix} &= \mu_k [v_1 \ \dots \ v_k \ v_{k+1}] \begin{bmatrix} h_{1k} \\ \vdots \\ h_{kk} - \eta_k/\mu_k \\ h_{k+1,k} \end{bmatrix}. \end{aligned}$$

162 The last equation reveals that the subdiagonal element ratio is $\frac{\mu_k h_{k+1,k}}{\nu_k h_{k+1,k}} = \frac{\mu_k}{\nu_k} = \xi_k$. \square

163 From Theorem 3.2 we obtain a Hessenberg pencil (H_n, K_n) , satisfying $Z_n = H_n K_n^{-1}$ with
 164 K_n nonsingular, which represents the projection

$$(3.3) \quad V_n^H A V_n K_n = H_n.$$

165 Such a Hessenberg pencil will be called proper if it has no subdiagonal elements $h_{i+1,i}$ and
 166 $k_{i+1,i}$ simultaneously zero. Theorem 3.2 implies that \underline{H}_n and \underline{K}_n are linked, their subdiagonal
 167 ratios reveal the poles of the rational Krylov subspace from which they originate. These ratios
 168 are, however, invariant when \underline{H}_n and \underline{K}_n are both multiplied with an upper-triangular matrix
 169 R from the right, illustrating that the Hessenberg pencil $(\underline{H}_n, \underline{K}_n)$ is not unique.

170 An implicit Q-theorem for matrix-pencils $(\underline{H}_n, \underline{K}_n)$ exists, if the poles and starting
 171 vector are chosen and the structure of the matrices in this pencil is fixed. If the structure of
 172 the matrices is chosen to be Hessenberg, then the implicit Q-theorem can be found in the
 173 dissertation of Berljafa [4], the paper by Berljafa et al. [5] and the paper of Camps et al. [8].

174 Theorem 3.3 states this result and shows a one-to-one relation between Hessenberg pencils
 175 and rational Krylov subspaces, therefore manipulating poles in the pencil corresponds to
 176 manipulating the subspaces.

THEOREM 3.3 (Rational implicit Q-theorem [4, 5, 8]). *Consider a decomposition of the form*

$$AV_{n+1}K_n = V_{n+1}H_n$$

177 with $(n+1) \times n$ Hessenberg matrices H_n and K_n , poles $\xi_i = \frac{h_{i+1,i}}{k_{i+1,i}}$, for $i = 1, \dots, n$ and
 178 V_{n+1} an orthonormal nested basis for the rational Krylov subspace $\mathcal{K}_{n+1}(A, v; \Xi)$, where
 179 $v = V_{n+1}e_1$ the first column of V_{n+1} and $\Xi = \{\xi_1, \xi_2, \dots, \xi_n\}$ the set of poles.

180 Then the Hessenberg pencil (H_n, K_n) and the orthonormal matrix V_{n+1} are essentially
 181 uniquely determined by the starting vector v and the poles Ξ .

182 Note that Theorem 3.3 states the uniqueness of the Hessenberg pencil. The pencil can,
 183 however, also be represented using matrices with another structure than Hessenberg. Since
 184 for a nonsingular matrix C the pair $(H_n C, K_n C)$ also satisfies (3.3). Besides the Hessenberg
 185 pencil, another important representation is an inv-Hessenberg pencil. This representation is
 186 discussed in Section 3.3 and is important for the derivation of the main result of this text
 187 provided in Section 4.

188 **3.3. Inv-Hessenberg pencil.** An inv-Hessenberg pencil satisfying (3.3) is constructed
 189 in this section.

190 PROPERTY 3.1 (Transfer through property [34]). *A shape of core transformations can be*
 191 *transferred through an upper-triangular matrix R without altering the shape.*

192 EXAMPLE 3.4. The equality $C_1 C_3 C_2 C_4 R = \tilde{R} \tilde{C}_1 \tilde{C}_3 \tilde{C}_2 \tilde{C}_4$ holds, where \tilde{R} is upper-
 193 triangular. The matrices involved will generally change (its elements), but the shape, i.e., the
 194 mutual ordering of the core transformations (and therefore the structure of the resulting matrix)
 195 remains the same.

LEMMA 3.5 (Turnover lemma [35], Lemma 9.38). *Consider the product of three core*
transformations $G_{i-1} G_i \hat{G}_{i-1}$. Then there exists an equivalent representation $\Gamma_i \Gamma_{i-1} \hat{\Gamma}_i$

$$\begin{array}{c} \updownarrow \\ \updownarrow \\ \updownarrow \end{array} = \begin{array}{c} \updownarrow \\ \updownarrow \\ \updownarrow \end{array}$$

$$G_{i-1} G_i \hat{G}_{i-1} = \Gamma_i \Gamma_{i-1} \hat{\Gamma}_i,$$

with matrices defined as

$$G_{i-1} := \begin{bmatrix} c_{i-1} & s_{i-1} & & \\ -s_{i-1} & c_{i-1} & & \\ & & & 1 \end{bmatrix} \quad G_i := \begin{bmatrix} 1 & & & \\ & c_i & s_i & \\ & -s_i & c_i & \\ & & & 1 \end{bmatrix} \quad \hat{G}_{i-1} := \begin{bmatrix} \hat{c}_{i-1} & \hat{s}_{i-1} & & \\ -\hat{s}_{i-1} & \hat{c}_{i-1} & & \\ & & & 1 \end{bmatrix}$$

$$\Gamma_i := \begin{bmatrix} 1 & & & \\ & \gamma_i & \sigma_i & \\ & -\sigma_i & \gamma_i & \\ & & & 1 \end{bmatrix} \quad \Gamma_{i-1} := \begin{bmatrix} \gamma_{i-1} & \sigma_{i-1} & & \\ -\sigma_{i-1} & \gamma_{i-1} & & \\ & & & 1 \end{bmatrix} \quad \hat{\Gamma}_i := \begin{bmatrix} 1 & & & \\ & \hat{\gamma}_i & \hat{\sigma}_i & \\ & -\hat{\sigma}_i & \hat{\gamma}_i & \\ & & & 1 \end{bmatrix}.$$

196 For ease of notation Theorem 3.6 is stated and proved for a full reduction ($n = m$) but is
 197 valid for partial reductions as well.

198 THEOREM 3.6 (Inv-Hessenberg pencil for projection onto rational Krylov subspaces).
 199 Let $V \in \mathbb{C}^{m \times m}$ be an orthonormal nested basis for a rational Krylov subspace $\mathcal{K}_m(A, v; \Xi)$,
 200 $A \in \mathbb{C}^{m \times m}$, $v \in \mathbb{C}^m$ and poles Ξ . Then the orthogonal projection onto this subspace
 201 can be represented as two inv-Hessenberg matrices H^{inv}, K^{inv} , i.e., they satisfy the equation
 202 $V^H A V K^{inv} = H^{inv}$.

Proof. The existence of a Hessenberg pair (H, K) satisfying

$$V^H AVK = H$$

follows immediately from the Arnoldi iteration in Theorem 3.2.

From Lemma 2.2 and Property 3.1 it follows that there exist upper-triangular matrices R_H and R_K and unitary matrices consisting of a descending pattern of core transformations Q_H and Q_K such that

$$V^H AVR_K Q_K = R_H Q_H.$$

203 Let us write it in a manner such that the structures are clear.

$V^H AV$ $\begin{matrix} \lceil \\ \lceil \\ \lceil \\ \dots \\ \lceil \end{matrix} = \begin{matrix} \lceil \\ \lceil \\ \lceil \\ \dots \\ \lceil \end{matrix}$

204

205 Multiply from the right with Q_K^H annihilate the descending pattern of core transformations on
 206 the left-hand side.

$V^H AV$ $= \begin{matrix} \lceil \\ \lceil \\ \lceil \\ \dots \\ \lceil \end{matrix}$

207

208 Using the turnover operation repeatedly, see [35] for details, it is possible to rearrange the core
 209 transformations to obtain another shape.

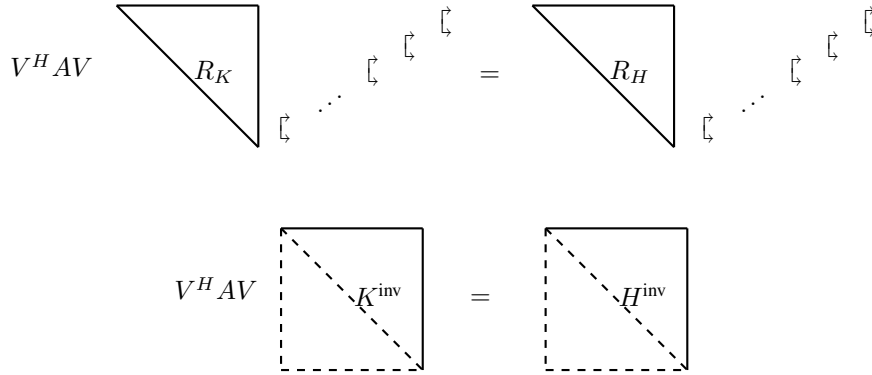
$V^H AV$ $= \begin{matrix} \lceil \\ \lceil \\ \lceil \\ \dots \\ \lceil \end{matrix}$

210

211 Multiplying from the right to annihilate the descending pattern of core transformations brings
 212 them back to the left-hand side.

213

214 Using the notation from before, where dashed lines indicate low-rank structure.



Hence, we have constructed an inv-Hessenberg pair (H^{inv}, K^{inv}) which satisfies the matrix equality

$$V^H AV K^{inv} = H^{inv}. \quad \square$$

215

216 **3.4. Connection to other factorizations.** Theorem 3.6, Theorem 3.2 and the result from Section 3.1 are summarized in Table 3.1. The structure of the single matrix representation also

| $V^H AV = Z$ | $V^H AV K = H$ | |
|--------------|----------------|--|
| | | |
| | | |

Table 3.1: Summary of structures following from orthogonal projections onto a rational Krylov subspace with basis V .

217

218 appeared in a paper by Mach et al. [21] and the Hessenberg pencil representation is a classical
 219 result by Ruhe [25]. These results about structure provide the tools for deriving the tridiagonal
 220 pencil representation of oblique projection onto rational Krylov subspaces in Section 4.

221 **4. Biorthogonal rational Krylov subspaces.** This section provides results concerning
 222 the possible structures of a biorthogonal projection onto rational Krylov subspaces [19].

223 Section 4.1 provides results for the single-matrix representation. The main result of that
 224 section has been proven for extended Krylov subspaces by Mach, et al. [22]. Section 4.2
 225 provides novel results concerning structure of the pencil representation, elegantly generalizing
 226 the tridiagonal structure obtained by nonhermitian Lanczos. Section 4.3 provides an overview
 227 of the structures which are generalized by the results in this section. Based on the tridiagonal
 228 pencil a Lanczos iteration for rational Krylov subspaces is developed in Section 5.

229 **4.1. Single-matrix representation.** The structure of a biorthogonal projection expressed
 230 as a single matrix $Z_n = W_n^H AV_n$ is given in Theorem 4.1. Here V_n and W_n are biorthogonal,

231 i.e., $W_n^H V_n = I$, bases for two rational Krylov subspaces $\mathcal{K}(A, v; \Xi)$ and $\mathcal{L}(A^H, w; \Phi)$, re-
 232 spectively, with $A \in \mathbb{C}^{m \times m}$, $v, w \in \mathbb{C}^m$ and Ξ, Φ two (possibly) independent sets of poles.

233 For the sake of readability the corresponding proof and all subsequent proofs are provided for
 234 a full reduction (i.e., $n = m$).

235 The structure of Z_n can be deduced using matrix factorizations rather than relying on orthogo-
 236 nality of the basisvectors for the subspaces, see, e.g., [17, 29, 36].

237

THEOREM 4.1 (Structure of biorthogonal projection in single-matrix representation).
*Consider $A \in \mathbb{C}^{m \times m}$ and rational Krylov subspaces $\mathcal{K}(A, v; \Xi)$ and $\mathcal{L}(A^H, w; \Phi)$ with
 biorthogonal bases $V, W \in \mathbb{C}^{m \times m}$, respectively. Ξ and Φ are two sets containing poles
 that are not in the spectrum of A . Under the assumption that no breakdowns occur, the
 biorthogonal projection*

$$W^H A V = Z,$$

238 where Z has the structure below its diagonal determined by the poles of \mathcal{K} and the structure
 239 above its diagonal determined by poles of \mathcal{L} .

Proof. A similar proof appears in [22]. The proof is added for completeness. Consider
 the matrices Z_V and Z_W

$$Z_V = \hat{V}^H A \hat{V}, \quad Z_W = \hat{W}^H A^H \hat{W},$$

where \hat{V} and \hat{W} are orthogonal bases for the rational Krylov subspaces $\mathcal{K}(A, v; \Xi)$ and
 $\mathcal{L}(A^H, w; \Phi)$, respectively, with $w^H v = 1$. In general for the orthogonal bases $\hat{W}^H \hat{V} \neq I$,
 taking the non-pivoted LR-decomposition of the matrix product $\hat{W}^H \hat{V}$ will allow us to
 construct biorthogonal bases V and W . The non-pivoted LR-decomposition, consisting of a
 lower triangular L and upper triangular R , will retain the nestedness of the bases \hat{V} and \hat{W}
 and will make the bases orthogonal to each other:

$$\begin{aligned} \hat{W}^H \hat{V} &= LR \\ \underbrace{L^{-1} \hat{W}^H}_{=: W^H} \underbrace{\hat{V} R^{-1}}_{=: V} &= I \\ W^H V &= I. \end{aligned}$$

This decomposition exists if and only if $\hat{W}^H \hat{V}$ is strongly nonsingular, otherwise it will break
 at the first singular principal minor. This break corresponds to a breakdown and is typical
 for biorthogonal methods. In this case the structural results hold up to the occurrence of the
 breakdown. The structure of Z can be derived as follows. First consider

$$\begin{aligned} AV &= VZ \\ A \underbrace{V R}_{\hat{V}} &= \underbrace{V R}_{\hat{V}} R^{-1} Z R \\ A \hat{V} &= \hat{V} \underbrace{R^{-1} Z R}_{Z_V} \end{aligned}$$

240 which provides the equality

$$(4.1) \quad Z = R Z_V R^{-1}.$$

Second consider the relations

$$\begin{aligned}
 A^H W &= W Z^H \\
 A^H \underbrace{W L^H}_{\hat{W}} &= \underbrace{W L^H}_{\hat{W}} \underbrace{L^{-H} Z^H L^H}_{Z_W} \\
 A^H \hat{W} &= \hat{W} \underbrace{L^{-H} Z^H L^H}_{Z_W}
 \end{aligned}$$

241 which provides the equality

$$(4.2) \quad Z^H = L^H Z_W L^{-H}.$$

242 Multiplication with an upper-triangular matrix preserves the structure in the lower triangular
 243 part. Hence, the structure of Z is the same as the structure of Z_V for the lower triangular
 244 part, following from (4.1). The structure of the upper triangular part of Z is the same as the
 245 structure of the lower triangular part of Z_W , following from (4.2). \square

246 Theorem 4.1 is illustrated by Example 4.2 for extended Krylov subspaces.

EXAMPLE 4.2. Consider $A \in \mathbb{C}^{8 \times 8}$ and extended Krylov subspaces

$$\mathcal{K}_8 = \text{span}\{v, Av, A^2v, A^3v, A^4v, A^{-1}v, A^5v, A^{-2}v\},$$

$$\mathcal{L}_8 = \text{span}\{w, (A^H)^{-1}w, A^H w, (A^H)^{-2}w, (A^H)^{-3}w, (A^H)^{-4}w, (A^H)^2w, (A^H)^3w\}.$$

247 Orthogonal projection onto these subspaces results in matrices Z_V for \mathcal{K}_8 and Z_W for \mathcal{L}_8
 248 and biorthogonal projection onto \mathcal{K}_8 and \mathcal{L}_8 results in Z . The structure of these matrices is shown
 249 in Figure 4.1. In case of rational Krylov subspaces we only have to include a diagonal matrix
 250 containing the poles. Note the extended Hessenberg structure for the orthogonal projections
 251 and the same structure appearing in the biorthogonal projection, but now below as well as
 252 above the diagonal. Black lines are added to highlight the structure.

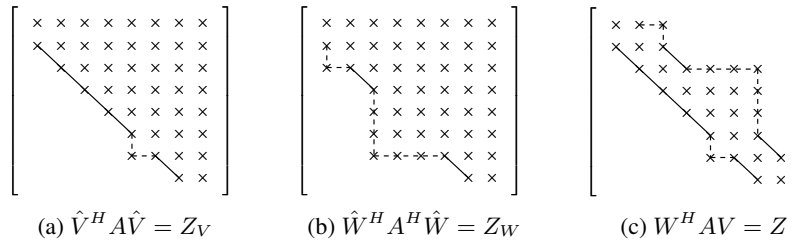


Fig. 4.1: Structure of orthogonal and biorthogonal projection onto the extended Krylov subspaces \mathcal{K}_8 and \mathcal{L}_8 in single-matrix representation, see Example 4.2.

253 The following lemma provides a result for unitary matrices stated by Bunse-Gerstner
 254 and Faßbender. [7], Stewart [31], and several others. It follows easily from Theorem 4.1 and
 255 illustrates how the theorem can be used as a general framework to derive structures arising
 256 from projection onto Krylov subspaces.

257 LEMMA 4.3. Consider a unitary matrix $U \in \mathbb{C}^{m \times m}$, some starting vector $v \in \mathbb{C}^m$
 258 and an orthogonal nested basis V for the standard Krylov subspace $\mathcal{K}_m(U, v)$. Under the
 259 assumption that no breakdown occurs, the projection $Z = V^H U V$ has Hessenberg structure
 260 below and inv-Hessenberg structure above the diagonal.

Proof. Consider a unitary matrix U , $U^{-1} = U^H$ and rational (more precisely extended) Krylov subspaces

$$\begin{aligned}\mathcal{K}(U, v; \Xi = \{\infty, \infty, \dots\}), \\ \mathcal{K}(U^H, v; \Phi = \{0, 0, \dots\}),\end{aligned}$$

with respective orthogonal bases \hat{V} and \hat{W} . Since $U^{-1} = U^H$, $\mathcal{K}(U, v; \Xi) = \mathcal{K}(U^H, v; \Phi) = \mathcal{K}(U, v)$ and therefore $\hat{V} = \hat{W} =: V$ implying $\hat{V}^H \hat{W} = V^H V = I$. Hence, they are simultaneously orthogonal and biorthogonal bases.

Using the knowledge from Section 3.1 it is clear that the structure of

$$\begin{aligned}Z_V &= \hat{V}^H A \hat{V}, \\ Z_W &= \hat{W}^H A^H \hat{W},\end{aligned}$$

261 is Hessenberg and inv-Hessenberg, respectively. Theorem 4.1 then states that $Z = \hat{W}^H A \hat{V} =$
 262 $V^H A V$ has Hessenberg structure in its lower triangular part and inv-Hessenberg structure in
 263 its upper triangular part. \square

264 Retrieving the poles of both spaces \mathcal{K} and \mathcal{L} from the single-matrix representation Z is
 265 possible but rather technical, especially in the parts where the matrix is not of Hessenberg
 266 form. Next section discusses the pencil representation which allows a more elegant retrieval
 267 of the poles in case a tridiagonal pencil is used.

268 **4.2. Pencil representation.** The main contribution of this text is the general pencil
 269 structure given in Theorem 4.4. A specific instance is a tridiagonal pencil, which is formulated
 270 in Lemma 4.5. As a consequence of the tridiagonal pencil a six-term recurrence relation can
 271 be derived for the biorthogonal bases for rational Krylov subspaces in Section 5.

THEOREM 4.4 (Pencil structure of biorthogonal projection onto rational Krylov subspaces). *Consider $A \in \mathbb{C}^{m \times m}$, two vectors $v, w \in \mathbb{C}^m$ and two rational Krylov subspaces $\mathcal{K}(A, v; \Xi)$ and $\mathcal{L}(A^H, w; \Psi)$, where Ξ and Ψ are two sets of poles (not in the spectrum of A). Let $\hat{V}, \hat{W} \in \mathbb{C}^{m \times m}$ be orthogonal nested bases and $V, W \in \mathbb{C}^{m \times m}$ biorthogonal nested bases for \mathcal{K} and \mathcal{L} , respectively. Then there exist H, K, H_V, K_V, H_W, K_W such that*

$$\begin{aligned}\hat{V}^H A \hat{V} K_V &= H_V \\ \hat{W}^H A^H \hat{W} K_W &= H_W \\ W^H A V K &= H\end{aligned}$$

272 and the structure of the pencil (H, K) is related to the structure of the pencils (H_V, K_V)
 273 and (H_W, K_W) . Inverted structure is short for writing that a Hessenberg block becomes an
 274 inv-hessenberg block and vice versa, then the structure can be related as

- 275 • H has the same structure below its diagonal as H_V and above its diagonal the
 276 inverted structure of K_W
- 277 • K has the same structure below its diagonal as K_V and above its diagonal the
 278 inverted structure of H_W .

Proof. From the orthogonal bases \hat{V} and \hat{W} , the biorthogonal bases V and W can be constructed as in Theorem 4.1, i.e., $V := \hat{V} R^{-1}$ and $W^H := L^{-1} \hat{W}^H$. Substituting the expressions for the biorthogonal bases in the equation of the orthogonal projection (3.3)

provides

$$\begin{aligned}
 & \begin{cases} A\hat{V}K_V = \hat{V}H_V \\ A^H\hat{W}K_W = \hat{W}H_W \end{cases} \\
 \Leftrightarrow & \begin{cases} A\hat{V}R^{-1}RK_V = \hat{V}R^{-1}RH_V \\ A^H\hat{W}L^{-H}L^HK_W = \hat{W}L^{-H}L^HH_W \end{cases} \\
 \Leftrightarrow & \begin{cases} AVRK_V = VRH_V \\ A^HWL^HK_W = WL^HH_W \end{cases} \\
 \Leftrightarrow & \begin{cases} W^H AVRK_V = RH_V \\ V^HA^HWL^HK_W = L^HH_W \end{cases} .
 \end{aligned}$$

Taking the Hermitian conjugate of the second equation and rewriting it reveals the connection between the matrices at play

$$\begin{cases} W^H AVRK_V = RH_V \\ W^H AVL^{-1}H_W^{-H} = L^{-1}K_W^{-H} \end{cases} .$$

Since these expressions are only unique up to right multiplication with a nonsingular matrix B , we get

$$\begin{aligned}
 RK_V B &= L^{-1}H_W^{-H} \\
 RH_V B &= L^{-1}K_W^{-H} .
 \end{aligned}$$

To obtain a particular choice for the structure of H and K it suffices to represent B in its RL -decomposition (assuming it exists), where R is an upper-triangular matrix and L a lower-triangular matrix

$$\begin{aligned}
 & \begin{cases} RK_V B = L^{-1}H_W^{-H} \\ RH_V B = L^{-1}K_W^{-H} \end{cases} \\
 \Leftrightarrow & \begin{cases} RK_V R_B L_B = L^{-1}H_W^{-H} \\ RH_V R_B L_B = L^{-1}K_W^{-H} \end{cases} \\
 \Leftrightarrow & \begin{cases} RK_V R_B = L^{-1}H_W^{-H} L_B^{-1} =: K \\ RH_V R_B = L^{-1}K_W^{-H} L_B^{-1} =: H \end{cases} .
 \end{aligned}$$

279 For the remainder of this proof H and K are defined as in the last equation. Other choices are
 280 possible because of the non-uniqueness of the pencil representation. Since R and R_B are upper-
 281 triangular matrices, they preserve the structure in the lower triangular part. This means that K
 282 and K_V have the same lower triangular structure and so do H and H_V . On the other hand K
 283 shares its upper triangular structure with H_W^{-H} and H with K_W^{-H} , since L and L_B are lower-
 284 triangular matrices. \square

285 Starting from Theorem 4.4 it is straightforward to prove the following lemma.

286 LEMMA 4.5 (Tridiagonal pencil for biorthogonal rational Krylov subspaces). *Consider*
 287 *some matrix* $A \in \mathbb{C}^{m \times m}$ *and vectors* $v, w \in \mathbb{C}^m$. *Let* $V, W \in \mathbb{C}^{m \times m}$ *be biorthogonal bases*
 288 *for rational Krylov subspaces* $\mathcal{K}(A, v; \Xi)$ *and* $\mathcal{L}(A^H, w; \Psi)$, *where the poles are not in the*
 289 *spectrum of* A . *The equation*

$$(4.3) \quad W^H AVS = T$$

290 representing the projection onto \mathcal{K} and orthogonal to \mathcal{L} is satisfied for a tridiagonal pencil
 291 (T, S) .

292 *Proof.* If (H_V, K_V) is chosen to be a Hessenberg pair (Theorem 3.2) and (H_W, K_W)
 293 to be an inv-Hessenberg pair (Theorem 3.6), then Theorem 4.4 guarantees that (T, S) has
 294 tridiagonal structure. \square

295 The pencil analogue to Lemma 4.3 can be derived from Theorem 4.4. This illustrates the
 296 ease with which structures in pencil form can be derived using this theorem. We stress that
 297 this result is only of theoretical use, not practical.

298 **LEMMA 4.6.** Consider a unitary matrix $U \in \mathbb{C}^{m \times m}$, some starting vector $v \in \mathbb{C}^m$
 299 and an orthogonal nested basis V for the standard Krylov subspace $\mathcal{K}(U, v)$. Under the
 300 assumption that no breakdown occurs, the equation $V^H U V K = H$ is satisfied for a proper
 301 lower-bidiagonal and upper-bidiagonal pencil (H, K) .

Proof. Consider a unitary matrix $U, U^{-1} = U^H$ and the same subspaces $\mathcal{K}(U, v; \Xi)$ and
 $\mathcal{K}(U^H, v; \Phi)$ as in the proof of Lemma 4.3, with respective orthogonal bases \hat{V} and \hat{W} , note
 that $\hat{V} = \hat{W} =: V$.

The pencil representation of orthogonal projections onto these subspaces are the following

$$\begin{aligned} \hat{V}^H U \hat{V} K_V &= H_V, \\ \hat{W}^H U^H \hat{W} K_W &= H_W. \end{aligned}$$

302 For (H_V, K_V) , consider the standard case: K_V is upper-triangular and H_V is of Hessenberg
 303 form. For (H_W, K_W) , choose H_W to be of inv-Hessenberg form and K_W to be upper-
 304 triangular. Then following from Theorem 4.4 the structure of (H, K) is a lower-bidiagonal
 305 and upper-bidiagonal pencil. \square

306 Lemma 4.6 together with Lemma 4.3 shows that a unitary Hessenberg matrix Z can be
 307 factorized as the product of a lower-bidiagonal matrix H and the inverse of an upper-bidiagonal
 308 matrix K [35], using the notation from the lemmas.

309 **4.3. Connection to other factorizations.** The results from this section generalize many
 310 well-known results such as the nonhermitian Lanczos iteration [19], the Hermitian rational
 311 Lanczos iteration [10], AGR- or CMV-factorization [36] and more recent results by Jagels and
 312 Reichel [17], Schweitzer [29], and others. Table 4.1 visualizes the structures of biorthogonal
 313 projection onto rational Krylov subspaces. The main contribution of this paper are the entries
 314 on the right, biorthogonal projection onto rational Krylov subspaces for pencil representation.
 315 Through Theorem 4.4 it is possible to relate the structures appearing in Table 3.1 to those in
 Table 4.1.

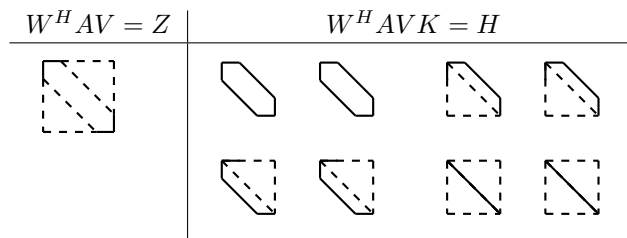


Table 4.1: Summary of pencil structures occurring for biorthogonal projections onto rational Krylov subspaces with bases V and W .

317 **5. Rational Lanczos iteration.** A Lanczos-type iteration which constructs biorthogonal
 318 bases for rational Krylov subspaces is tested in this section. Section 5.1 states results con-
 319 cerning the appearance of the poles of rational Krylov subspaces as ratios in the tridiagonal
 320 pencil (4.3). These results allow for the development of the Lanczos-type iteration, code
 321 implementing this iteration is included as an attachment. Some numerical results for this
 322 iteration are given in Section 5.2, these serve as a proof of concept, we have not yet focused
 323 on numerical stability.

324 **5.1. Lanczos-type iteration.** For the construction of a Lanczos-type iteration we must
 325 know how the poles appear in the tridiagonal pencil (4.3), Lemma 5.1 and Lemma 5.2 state
 326 this.

327 **LEMMA 5.1.** *Assume we have $W^H AVS = T$ as in Theorem 4.4. The ratio of the*
 328 *subdiagonal elements of (T, S) reveals the poles $\Xi = \{\xi_1, \xi_2, \dots, \xi_{m-1}\}$ of $\mathcal{K}(A, v; \Xi)$*

$$(5.1) \quad \frac{T_{i+1,i}}{S_{i+1,i}} = \xi_i, \quad i = 1, 2, \dots, m-1.$$

Proof. From Theorem 3.2 it follows that the ratio of the subdiagonal elements of
 (H_V, K_V) equals the poles

$$\frac{(H_V)_{i+1,i}}{(K_V)_{i+1,i}} = \xi_i, \quad i = 1, 2, \dots, m-1,$$

and since

$$\frac{T_{i+1,i}}{S_{i+1,i}} = \frac{R_{i+1,i+1}(H_V)_{i+1,i}(R_B)_{ii}}{R_{i+1,i+1}(K_V)_{i+1,i}(R_B)_{ii}} = \frac{(H_V)_{i+1,i}}{(K_V)_{i+1,i}}, \quad i = 1, 2, \dots, m-1,$$

329 where in the first equality we used a result stated in the proof of Theorem 4.4 with R and R_B
 330 upper-triangular matrices. \square

331 **LEMMA 5.2.** *Let (T, S) be the tridiagonal pencil satisfying (4.3). The ratio of the super-*
 332 *diagonal elements of (T, S) reveals the (complex conjugate of the) poles $\Psi = \{\psi_1, \psi_2, \dots, \psi_{m-2}\}$*
 333 *of $\mathcal{L}(A^H, w; \Psi)$*
 334

$$(5.2) \quad \frac{T_{i,i+1}}{S_{i,i+1}} = \bar{\psi}_{i-1}, \quad i = 2, 3, \dots, m-1.$$

335 *Proof.* Assume we have $W^H AVS = T$ as in Theorem 4.4. Note that another tridiagonal
 336 pencil (\tilde{S}, \tilde{T}) exists for which

$$(5.3) \quad V^H A^H W \tilde{T} = \tilde{S}.$$

Equation (4.3) represents projection onto \mathcal{K} and orthogonal to \mathcal{L} and Equation (5.3) represents
 projection onto \mathcal{L} and orthogonal to \mathcal{K} . Hence, from Lemma 5.1 we know that the ratios of
 the subdiagonals of (T, S) and (\tilde{S}, \tilde{T}) reveal the poles of \mathcal{K} and \mathcal{L} , respectively.
 Starting from Equation (4.3) and (5.3) we can relate the matrix pencils as follows

$$\begin{cases} W^H AV = TS^{-1} \\ V^H A^H W = \tilde{S}\tilde{T}^{-1} \end{cases} \Rightarrow \begin{cases} W^H AV = TS^{-1} \\ W^H AV = \tilde{T}^{-H}\tilde{S}^H \end{cases}$$

concluding that $TS^{-1} = \tilde{T}^{-H}\tilde{S}^H$. Rewriting this equation as $\tilde{T}^H T = \tilde{S}^H S$ leads to two
 pentadiagonal matrices. Let us assign a variable to each off-diagonal element, diagonal

elements are marked as an x, because these are not relevant for the proof

$$\begin{bmatrix} \times & \tilde{\tau}_1 & & & \\ \tilde{t}_1 & \times & \tilde{\tau}_2 & & \\ & \tilde{t}_2 & \times & \ddots & \\ & & \ddots & \ddots & \tilde{\tau}_{n-1} \\ & & & \tilde{t}_{n-1} & \times \end{bmatrix}^H = \begin{bmatrix} \times & \tau_1 & & & \\ t_1 & \times & \tau_2 & & \\ & t_2 & \times & \ddots & \\ & & \ddots & \ddots & \tau_{n-1} \\ & & & t_{n-1} & \times \end{bmatrix} = \begin{bmatrix} \times & \tilde{\sigma}_1 & & & \\ \tilde{s}_1 & \times & \tilde{\sigma}_2 & & \\ & \tilde{s}_2 & \times & \ddots & \\ & & \ddots & \ddots & \tilde{\sigma}_{n-1} \\ & & & \tilde{s}_{n-1} & \times \end{bmatrix}^H = \begin{bmatrix} \times & \sigma_1 & & & \\ s_1 & \times & \sigma_2 & & \\ & s_2 & \times & \ddots & \\ & & \ddots & \ddots & \sigma_{n-1} \\ & & & s_{n-1} & \times \end{bmatrix}.$$

Hence, by equating the second superdiagonals and second subdiagonals of both pentadiagonal matrices we get

$$\begin{cases} t_i \tilde{\tau}_{i+1}^H = s_i \tilde{\sigma}_{i+1}^H \\ \tau_{i+1} \tilde{t}_i^H = \sigma_{i+1} \tilde{s}_i^H \end{cases}, \quad i = 1, \dots, m-2 \\
 \Rightarrow \begin{cases} \xi_i = t_i/s_i = \tilde{\sigma}_{i+1}^H/\tilde{\tau}_{i+1}^H \\ \psi_i = \tilde{s}_i/\tilde{t}_i = \tau_{i+1}^H/\sigma_{i+1}^H \end{cases}, \quad i = 1, \dots, m-2.$$

337 where the last equality uses the result from Lemma 5.1. \square

338

339 Note that Lemma 5.2 allows for freedom in the choice of $T_{1,2}$ and $S_{1,2}$. The results from
 340 Theorem 4.5, Lemma 5.1 and Lemma 5.2 can be used to construct a six-term recurrence
 341 relation, which builds biorthogonal bases for rational Krylov subspaces. This is the Lanczos-
 342 type iteration, code is included which implements this. The derivation of the iteration is
 343 omitted since it is straightforward but lengthy.

344 **5.2. Numerical experiments.** The validity of the Lanczos-type iteration is verified by
 345 applying it to solve an eigenvalue problem. Three characteristics of the algorithm will be
 346 monitored:

- 347 • $\|W_n^H V_n - I\|_2$, a measure for the biorthogonality of bases W and V ,
- 348 • $\|W_{n+1}^H A V_{n+1} S_n - T_n\|_2$, a measure for the quality of the oblique projection and,
- 349 • a Ritz plot visualizing the quality of Ritz values as approximations to eigenvalues.

The projection measure uses the expansion matrices $(\underline{T}_n, \underline{S}_n)$ resulting from the Lanczos iteration, i.e., they are of dimension $(n+1) \times n$. We compare the Ritz values $\theta^{(n)}$ of (T_n, S_n) , last row of $(\underline{T}_n, \underline{S}_n)$ removed, with the eigenvalues λ of A . Ritz plots visualize how close the n Ritz values $\theta_i^{(n)}$, $1 \leq i \leq n$, are to the closest eigenvalue $\lambda_i := \min_{\lambda} |\theta_i^{(n)} - \lambda|$ for increasing n . The colours show how accurate the approximation is:

$$\begin{aligned}
 \text{red: } & \|\theta_i^{(n)} - \lambda_i\|_2 < 10^{-8}, \\
 \text{yellow: } & \|\theta_i^{(n)} - \lambda_i\|_2 < 10^{-5}, \\
 \text{green: } & \|\theta_i^{(n)} - \lambda_i\|_2 < 10^{-2}, \\
 \text{blue: } & \|\theta_i^{(n)} - \lambda_i\|_2 \geq 10^{-2}.
 \end{aligned}$$

350 **EXAMPLE 5.3.** Consider a random 50×50 upper triangular matrix with eigenvalues
 351 $\lambda_i = i, i = 1, 2, \dots, 50$. Krylov subspaces $\mathcal{K}(A, v; \Xi)$ and $\mathcal{L}(A^H, w; \Phi)$ are build using
 352 $v = w$ and $\Xi = \Phi = \{0, 24.1, 0, 24.1, \dots\}$. Biorthogonal projection using these subspaces
 353 lead to Figure 5.1a for the biorthogonality measure, Figure 5.1b for the measure quantifying
 354 the projection (T, S) and Figure 5.2 showing the Ritz plot. The Ritz plot clearly shows
 355 that convergence is concentrated around the chosen poles 0 and 24.1. This is the expected
 356 behaviour, the convergence of rational Krylov methods can be focussed on certain parts of the
 357 spectrum [25].

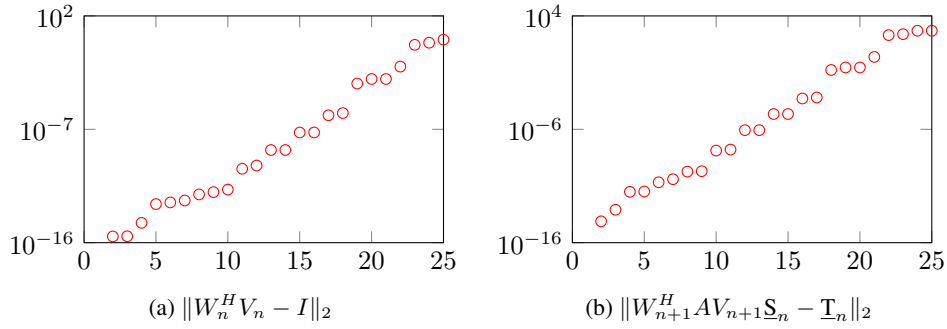


Fig. 5.1: Measures for Example 5.3, with n the dimension of the rational Krylov subspaces.

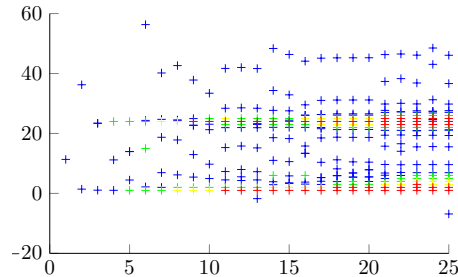


Fig. 5.2: Ritz plot for Example 5.3, with n the dimension of the rational Krylov subspaces.

358 **EXAMPLE 5.4.** To show the connection between convergence of eigenvalues and biorthog-
 359 onality, we choose a pole closer to an eigenvalue. This leads to faster convergence to
 360 this eigenvalue and thus to faster loss of biorthogonality [24]. The poles chosen now are
 361 $\Xi = \Phi = \{0, 24 + 10^{-5}, 0, 24 + 10^{-5}, \dots\}$. Figure 5.4 shows that eigenvalue $\lambda = 24$ is
 362 found in fewer iterations than in Example 5.3. This leads to faster loss of biorthogonality of
 363 the bases, shown on Figure 5.3a. Figure 5.3b shows that the quality of the projection is related
 364 to the biorthogonality of the bases.

365 Note that we did not use examples where $\Xi \neq \Phi$, since the behaviour of such choices is
 366 not comparable with any existing Lanczos-type iterations and subject to future research. From
 367 Example 5.3 and Example 5.4 we conclude that the novel Lanczos-type iteration exhibits the
 368 expected behaviour, i.e., comparable to the behaviour of known iterations. Hence, the validity

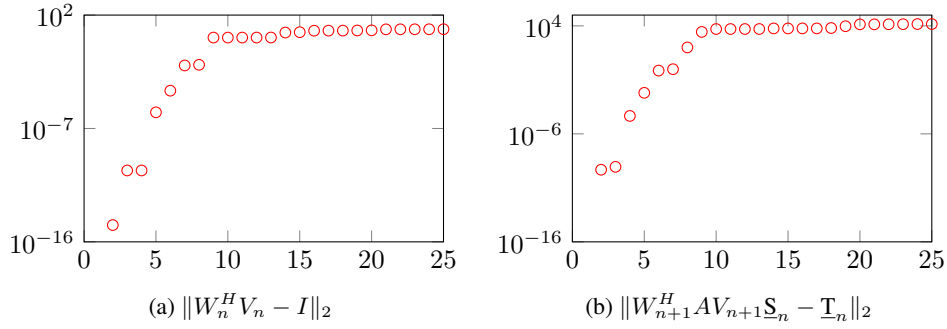


Fig. 5.3: Measures for Example 5.4, with n the dimension of the rational Krylov subspaces.

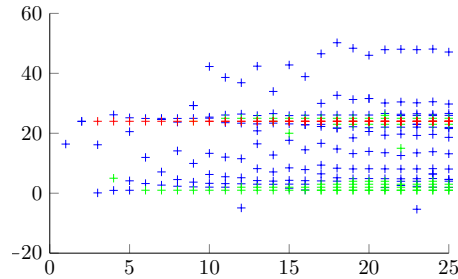


Fig. 5.4: Ritz plot for Example 5.4, with n the dimension of the rational Krylov subspaces.

369 of the rational Lanczos iteration is substantiated.

370 **6. Conclusion.** A general framework to predict the various structures arising in the
 371 context of rational Krylov subspace methods is developed. From this framework a pair of short
 372 recurrence relations for biorthogonal bases of rational Krylov subspaces is deduced. Based on
 373 the short recurrence relation a Lanczos-type iteration is derived which constructs these bases
 374 together with a tridiagonal pencil representing the obliquely projected matrix. The framework
 375 generalizes many classical and more recent results, as does the novel rational Lanczos iteration.
 376 Numerical tests are performed as a proof of concept for the iteration.

377 **7. Future Research.** A proper analysis of the numerical behaviour of the Lanczos
 378 iteration could provide the means to make it more stable.
 379 Furthermore the relation between biorthogonal rational Krylov subspaces and biorthogonal
 380 functions will be looked into.

381

REFERENCES

- 382 [1] G. AMMAR, W. GRAGG, AND L. REICHEL, *On the eigenproblem for orthogonal matrices*, in Decision and
 383 Control, 1986 25th IEEE Conference on, vol. 25, IEEE, 1986, pp. 1963–1966.
- 384 [2] W. E. ARNOLDI, *The principle of minimized iterations in the solution of the matrix eigenvalue problem*,
 385 Quarterly of Applied Mathematics, 9 (1951), pp. 17–29.
- 386 [3] J. L. AURENTZ, T. MACH, L. ROBOL, R. VANDEBRIL, AND D. S. WATKINS, *Core-chasing algorithms for
 387 the eigenvalue problem*.
- 388 [4] M. BERLJAJA, *Rational Krylov Decompositions: Theory and Applications*, PhD thesis, The University of
 389 Manchester, 2017.
- 390 [5] M. BERLJAJA AND GÜ, *Generalized rational Krylov decompositions with an application to rational approxi-
 391 mation*.
- 392 [6] A. BUNSE-GERSTNER AND L. ELSNER, *Schur parameter pencils for the solution of the unitary eigenproblem*,
 393 Linear Algebra and its Applications, 154 (1991), pp. 741–778.
- 394 [7] A. BUNSE-GERSTNER AND H. FASSBENDER, *Error bounds in the isometric Arnoldi process*, Journal of
 395 Computational and Applied Mathematics, 86 (1997), pp. 53–72.
- 396 [8] D. CAMPS, K. MEERBERGEN, AND R. VANDEBRIL, *An implicit filter for rational Krylov using core
 397 transformations*, Linear Algebra and its Applications, 561 (2019), pp. 113 – 140.
- 398 [9] M. J. CANTERO, L. MORAL, AND L. VELÁZQUEZ, *Five-diagonal matrices and zeros of orthogonal polyno-
 399 mials on the unit circle*, Linear Algebra and its Applications, 362 (2003), pp. 29–56.
- 400 [10] K. DECKERS AND A. BULTHEEL, *Rational Krylov sequences and orthogonal rational functions*, TW Reports,
 401 (2007).
- 402 [11] K. GALLIVAN, E. GRIMME, AND P. VAN DOOREN, *Padé approximation of large-scale dynamic systems with
 403 Lanczos methods*, in Proceedings of 1994 33rd IEEE Conference on Decision and Control, vol. 1, IEEE,
 404 1994, pp. 443–448.
- 405 [12] K. GALLIVAN, G. GRIMME, AND P. VAN DOOREN, *A rational Lanczos algorithm for model reduction*,
 406 Numerical Algorithms, 12 (1996), pp. 33–63.
- 407 [13] E. GRIMME, *Krylov projection methods for model reduction*, PhD thesis, University of Illinois at Urbana
 408 Champaign, 1997.
- 409 [14] M. H. GUTKNECHT, *Stationary and almost stationary iterative (k,l)-step methods for linear and nonlinear
 410 systems of equations*, Numerische Mathematik, 56 (1989), pp. 179–213.
- 411 [15] ———, *Lanczos-type solvers for nonsymmetric linear systems of equations*, Acta Numerica, 6 (1997), pp. 271–
 412 397.
- 413 [16] ———, *Revisiting (k,l)-step methods*, Numerical Algorithms, 69 (2015), pp. 455–469.
- 414 [17] C. JAGELS AND L. REICHEL, *Recursion relations for the extended Krylov subspace method*, Linear Algebra
 415 and its Applications, 434 (2011), pp. 1716–1732.
- 416 [18] A. N. KRYLOV, *On the numerical solution of the equation by which the frequency of small oscillations is
 417 determined in technical problems*, Izvestiya Akad. Nauk. SSSR, Ser. Fiz.-Mat., 4 (1931), pp. 491–539.
 418 In Russian.
- 419 [19] C. LANCZOS, *An iteration method for the solution of the eigenvalue problem of linear differential and integral
 420 operators*, Journal of Research of the National Bureau of Standards, 45 (1950), pp. 255–282.
- 421 [20] J. LIESEN AND Z. STRAKOŠ, *Krylov Subspace Methods: Principles and Analysis*, Oxford University Press,
 422 2013.
- 423 [21] T. MACH, M. S. PRANIĆ, AND R. VANDEBRIL, *Computing approximate (block) rational Krylov subspaces
 424 without explicit inversion with extensions to symmetric matrices*, Electron. Trans. Numer. Anal., 43 (2014),
 425 pp. 100–124.
- 426 [22] T. MACH, M. VAN BAREL, AND R. VANDEBRIL, *Inverse eigenvalue problems for extended Hessenberg
 427 and extended tridiagonal matrices*, Journal of Computational and Applied Mathematics, 272 (2014),
 428 pp. 377–398.
- 429 [23] C. MERTENS AND R. VANDEBRIL, *Short recurrences for computing extended Krylov bases for Hermitian and
 430 unitary matrices*, Numerische Mathematik, 131 (2015), pp. 303–328.
- 431 [24] C. C. PAIGE, *The computation of eigenvalues and eigenvectors of very large sparse matrices.*, PhD thesis,
 432 University of London, 1971.
- 433 [25] A. RUHE, *Rational Krylov sequence methods for eigenvalue computation*, Linear Algebra and its Applications,
 434 58 (1984), pp. 391–405.
- 435 [26] ———, *Rational Krylov algorithms for nonsymmetric eigenvalue problems. II. Matrix pairs*, Linear algebra
 436 and its Applications, 197 (1994), pp. 283–295.
- 437 [27] Y. SAAD, *Numerical Methods for Large Eigenvalue Problems*, Algorithms and Architectures for Advanced
 438 Scientific Computing, Manchester University Press, Manchester, 1992.
- 439 [28] Y. SAAD, *Iterative Methods for Sparse Linear Systems*, SIAM, 2003.
- 440 [29] M. SCHWEITZER, *A two-sided short-recurrence extended Krylov subspace method for nonsymmetric matrices
 441 and its relation to rational moment matching*, Numerical Algorithms, 76 (2017), pp. 1–31.

- 442 [30] B. SIMON, *CMV matrices: Five years after*, Journal of Computational and Applied Mathematics, 208 (2007),
443 pp. 120–154.
- 444 [31] M. STEWART, *A generalized isometric Arnoldi algorithm*, Linear Algebra and its Applications, 423 (2007),
445 pp. 183–208.
- 446 [32] H. A. VAN DER VORST, *BiCGSTAB a fast and smoothly converging variant of BiCG for the solution of*
447 *nonsymmetric linear systems*, SIAM Journal on Statistical Computing, 13 (1992), pp. 631–644.
- 448 [33] H. A. VAN DER VORST, *Iterative Krylov Methods for Large Linear Systems*, Cambridge University Press,
449 2003.
- 450 [34] R. VANDEBRIL, *Chasing bulges or rotations? A metamorphosis of the QR-algorithm*, SIAM Journal on Matrix
451 Analysis and Applications, 32 (2011), pp. 217–247.
- 452 [35] R. VANDEBRIL, M. VAN BAREL, AND N. MASTRONARDI, *Matrix Computations and Semiseparable Matrices:*
453 *Linear Systems*, vol. 1, John Hopkins University Press, 2007.
- 454 [36] D. S. WATKINS, *Some perspectives on the eigenvalue problem*, SIAM Review, 35 (1993), pp. 430–471.